A bimetallic-activated MnO_2 self-assembly electrode with a dual heterojunction structure for high-performance rechargeable zinc-air batteries

Zhengyu Yin[1,#], Rui He[1,#], Huaibin Xue[2], Jingjian Chen[1], Yue Wang[1], Xiaoxiao Ye[1], Nengneng Xu[1,*], Jinli Qiao[1,3,*], Haitao Huang[4,*]

[1]State Key Laboratory for Modification of Chemical Fibers and Polymer Materials, College of Environmental Science and Engineering, Donghua University, Shanghai 201620, China.

[2]Shanghai Jinyuyuan Clean-Energy Technology Co., Ltd., Shanghai 201208 China.

[3]Shanghai Institute of Pollution Control and Ecological Security, Shanghai 200092, China.

[4]Department of Applied Physics, Hong Kong Polytechnic University, Hong Kong, China.

[#]Authors contributed equally.

***Correspondence to**: Prof. Jinli-Qiao, State Key Laboratory for Modification of Chemical Fibers and Polymer Materials, College of Environmental Science and Engineering, Donghua University, 2999 Ren'min North Road, Shanghai 201620, China. E-mail: qiaojl@dhu.edu.cn; Dr. Nengneng Xu, College of Environmental Science and Engineering, Donghua University, 2999 Ren'min North Road, Shanghai 201620, China. E-mail: nengnengxu@dhu.edu.cn; Prof. Haitao Huang, Department of Applied Physics, Hong Kong Polytechnic University, 11 yucai road, Kowloon, Hongkong, China. E-mail: aphhuang@polyu.edu.hk.

EXPERIMENTAL

Materials and catalyst preparation

The self-supported electrode was synthesized through a facial hydrothermal self-assembly process and a calcination treatment. In a typical synthesis, 0.79 g $KMnO_4$ and 2 mL HCl (36 wt%) were added to 50 mL deionized (D.I.) water to form a precursor solution. Then the mixture was transferred into a 100 mL Teflon-lined stainless steel autoclave. The hydrothermal reaction was carried out at 140 °C for 12 hours. After that the MnO_2 nanotubes was collected by centrifugation and washed with ethanol and D.I. water before vacuum-drying. The hybrid $NiCo_2O_4$@MnO_2/CNTs-Ni foam electrode was prepared by dissolving 0.250 g cobalt (II) acetate tetrahydrate and 0.250 g nickel acetate tetrahydrate in 30 mL (25-28 wt%) ammonia solution. Then, 0.2 g of as-prepared MnO_2 and 0.02 g CNTs were added to the above solution, with 0.5 h ultrasonic condition to form a uniform solution. Ni foam (2 cm x 2 cm) was cleaned under ultrasonication for every 30 min with D.I. water, 0.1M HCI and ethanol in order to remove the oxidized surface layer.Then the mixture solution and the preprocessed Ni foam were moved into a 100 mL autoclave and maintaining 160 °C for 6 h.The self-supporting electrode and resulting product were separated and washed with D.I. water. After that drying in a vacuum oven at 70 °C for 8 h. Finally, the resulting product and self-supporting electrode were further calcined in air at 350 °C for 1 h to obtain the target samples.

Physical characterizations of self-supporting air cathode

The morphologies of catalyst and electrode samples were assessed by an S-4800 field-emission scanning electron microscope (SEM). Transmission electron microscopy (TEM) evaluation were performed with a high-resolution Talos F200S to get information of the the dispersion and the particle size of the catalyst at 200 kV operating voltage. X-ray diffraction (XRD, Bruker D8 ADVANCE) was performed to analyze the crystallite phase and structure of the obtained samples over the 2θ range from 10° to 90°. X-ray photoelectron spectroscopy (XPS, Escalab 250Xi) was carried out to characterize the chemical states and the compositions of samples.

Electrode Preparation and Electrochemical Measurements

OER and ORR catalytic performance of the as-prepared catalyst powder samples and a self-supproting electrode were tested by the rotating disc electrode (RDE). Nafion as a binder impregnated in the catalyst ink and help the catalyst to be loaded on a glassy carbon disk electrode.

During the preparation of the powder catalyst ink, 10 mg of the as-prepared catalyst was added into 2 mL ethanol with16 μL 5 wt% Nafifion mixture solution. Form a well-dispersed catalyst ink by sonication. In the test, 16 μL of the catalyst ink was dropped onto the glassy carbon disk electrode. The catalyst loading content was controled in 2 mg cm^{-2}.The self- supproting electrode was prepared as 1 cm x 1cm size in the half-cell test. Electrochemical activity of the samples was studied using a linear sweep voltammetry (LSV). In the measurements, the glassy carbon disk electrode coating the catalyst was submerged in a five-port electrolytic cell containing 0.1 M KOH aqueous electrolyte, in which a platinum foil and a saturated calomel electrode (SCE) were used as the counter and reference electrodes, respectively. Then, LSV was performed with a potential range of 0.2V - 1.0 V vs reversible hydrogen electrode (RHE, φ(RHE)=φ(SCE)+0.24V+0.0591*pH) for ORR at 5 mV s^{-1} and a rotation rate of 400, 625, 900, 1225, and 1600 rpm and a potential range of 1.0 V - 2 V vs RHE for OER at 5 mV s^{-1} and a rotation rate of 1600 rpm. The transferred electron number of ORR was calculated from the slopes of Koutecky−Levich (K−L) plots[26]. A commercial Pt/C-RuO_2 catalyst was used as the comparative sample and tested using the same procedure as that for the self- supproting electrode except no rotating speed.

Performance measurements of ZABs

A rechargeable ZAB contains the following parts an air electrode (4 cm x 4 cm) loading 1 cm^2 catalyst and the $NiCo_2O_4$@MnO_2/CNTs-Ni foam self-supporting electrode were used as the air cathode. Zinc plate was used as the anode. 6 M KOH worked as the flowing electrolyte in the zinc-air battery.Power density plots were measured by galvanodynamic method. The rate capability of the ZAB assessed by

analyzing the galvanostatic discharge curves at different current densities from 5 to 30 mA cm^{-2}, with a growth rate of 5 mA cm^{-2}. The long-term stability of the ZAB was tested by constant current charge and discharge at 5 mA cm^{-2}, 20 min per cycle.

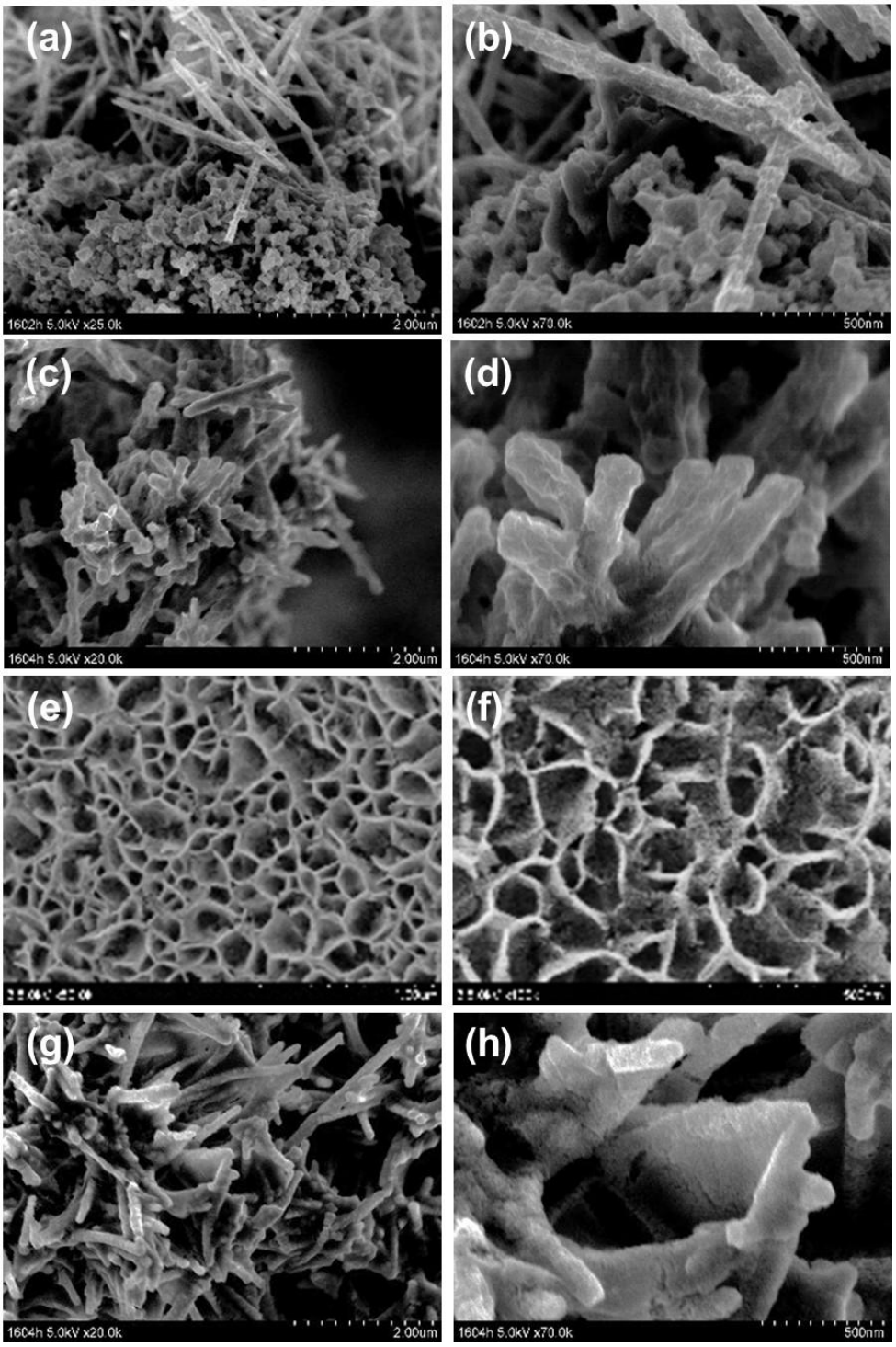

Supplementary Figure 1. SEM images of the $NiCo_2O_4$@MnO_2/CNTs-Ni foam obtained at 160 ºC (a and b) for 2 hours; (c and d) for 4hours; (e and f) for 6 hours; (g and h) for 8 hours.

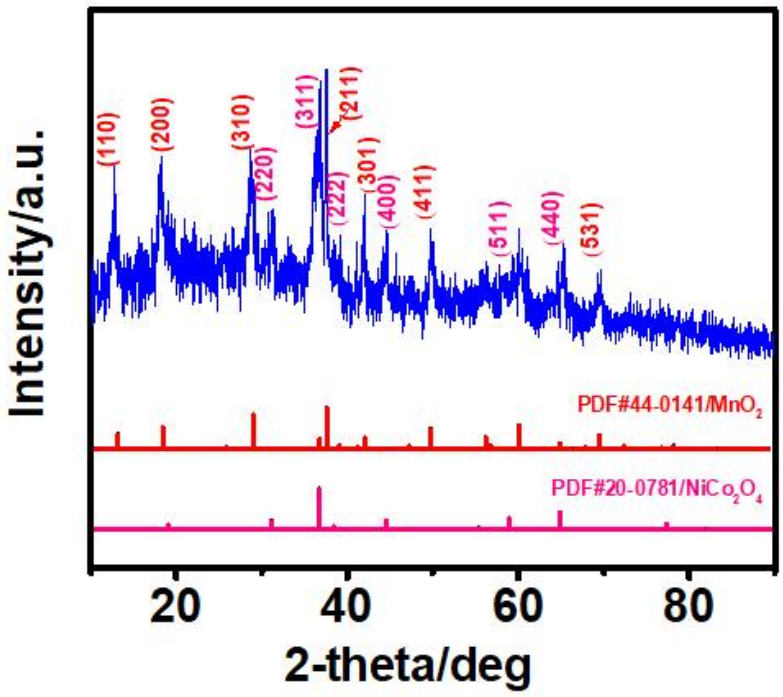

90 Supplementary Figure 2. XRD images of the $NiCo_2O_4$@MnO_2/CNTs-Ni foam.

91

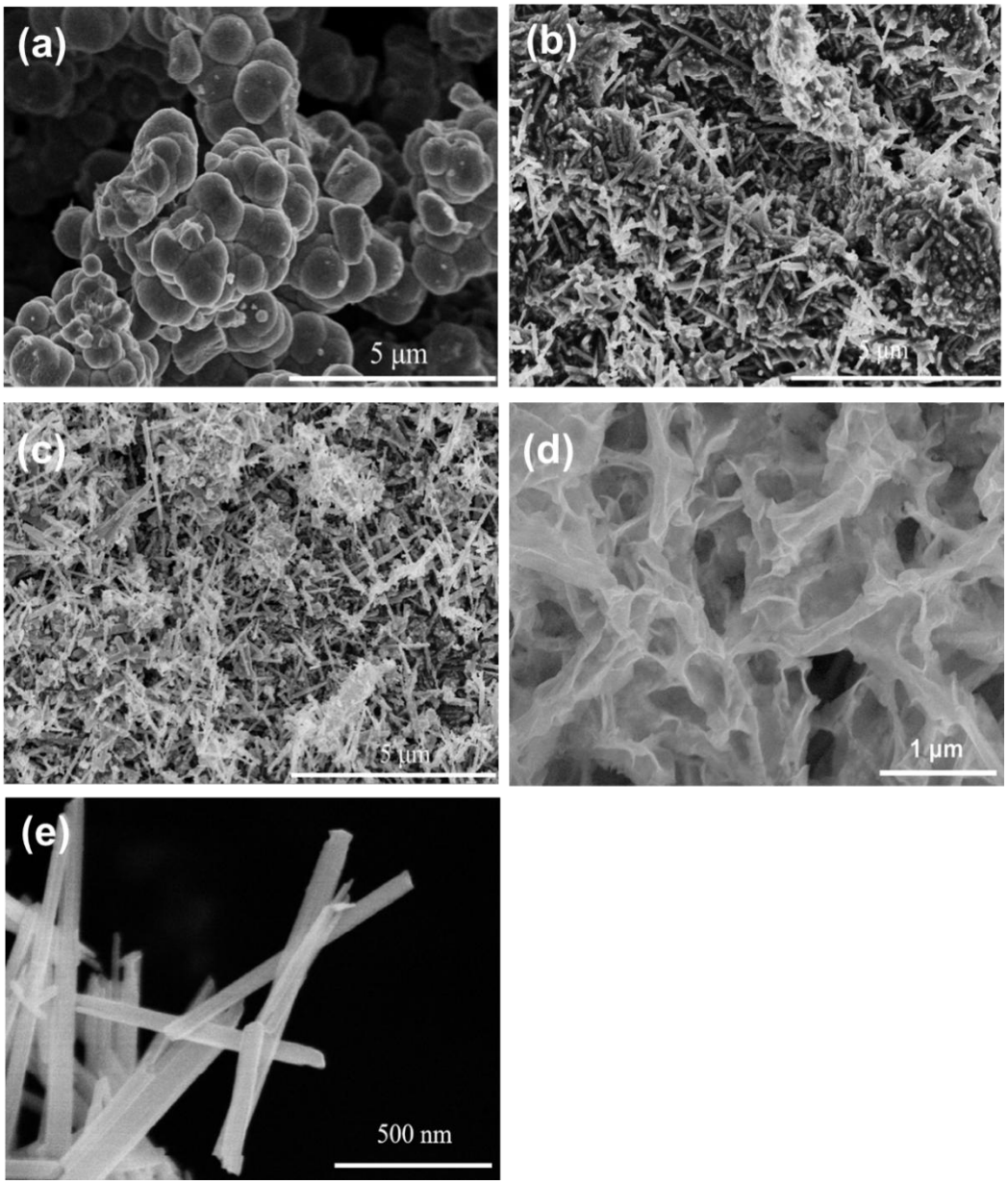

Supplementary Figure 3. SEM images of (a) $NiCo_2O_4$; (b) $NiCo_2O_4/MnO_2$-CNTs; (c) Co_3O_4/MnO_2-CNTs; (d) Co_3O_4@MnO_2-CNTs@Ni foam; (e) pure MnO_2.

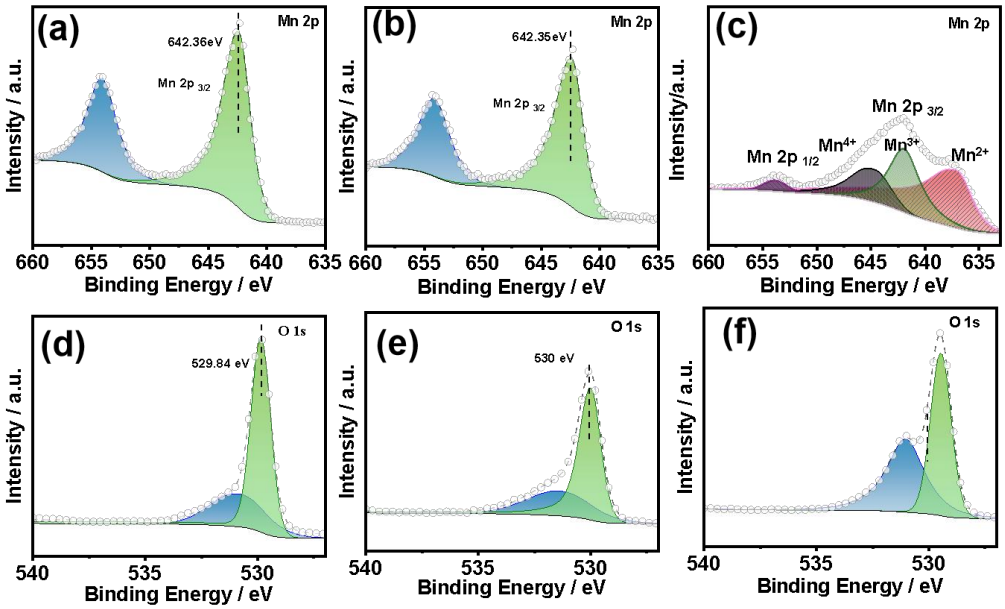

Supplementary Figure 4. High-resolution XPS curves of Mn 2p region for (a) pure MnO_2; (b)$NiCo_2O_4$/MnO_2-CNTs; (c) Co_3O_4@MnO_2-CNTs@Ni foam; High-resolution XPS curves of O 2p region for (d) pure MnO_2; (e)$NiCo_2O_4$/MnO_2-CNTs; (f) Co_3O_4@MnO_2-CNTs@Ni foam.

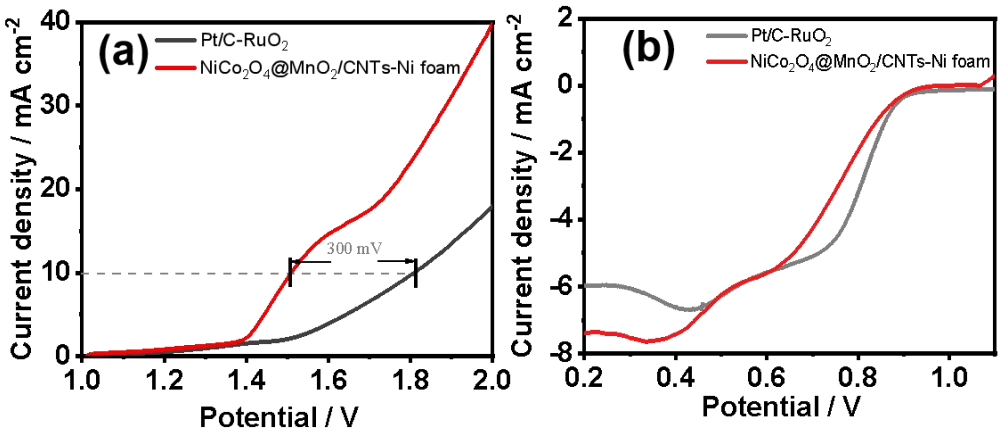

Supplementary Figure 5. Pt/C-RuO_2, $NiCo_2O_4$@MnO_2/CNTs-Ni foam (a) OER curves, (b) ORR curves.

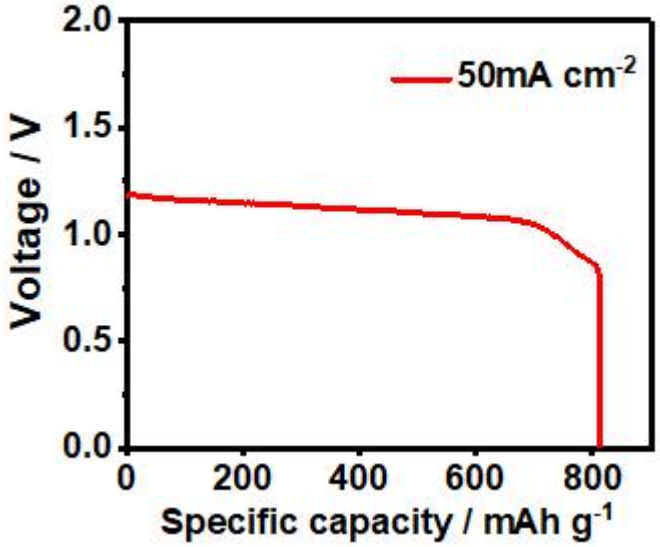

Supplementary Figure 6. The specific capacity of ZABs with $NiCo_2O_4$@MnO_2/CNTs-Ni foam cathode

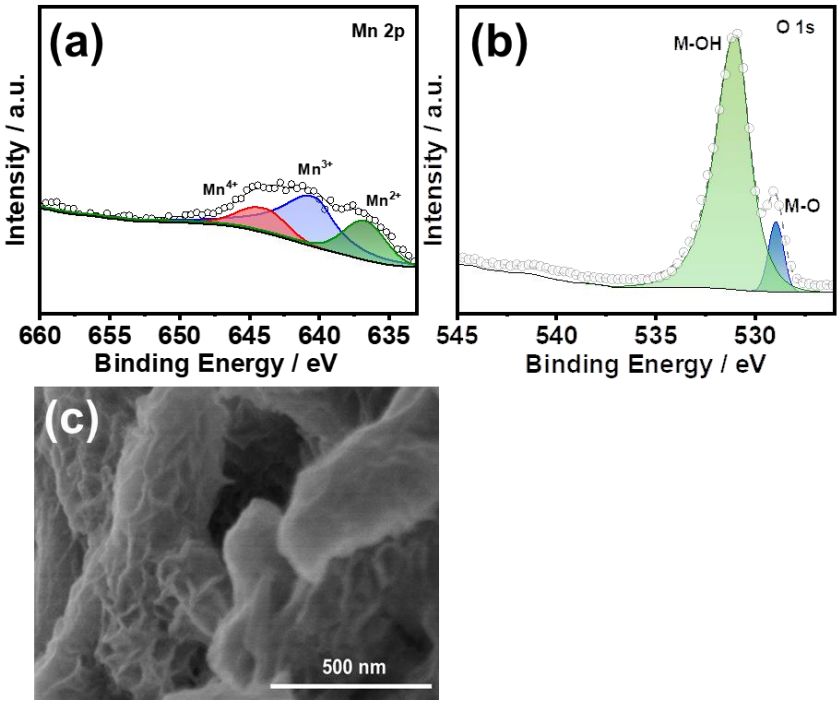

Supplementary Figure 7. Physical characterization of $NiCo_2O_4$@MnO_2/CNTs-Ni foam electrode after reaction long-term stability testing (a and b) XPS curves of Mn 2p and O 1s;(c) SEM image of tested $NiCo_2O_4$@MnO_2/CNTs-Ni foam electrode.

Table S1. The power density and voltage gaps are compared with several different types of MnO_2 and transition metal supported MnO_2.

Catalyst	Voltage gaps	Power density (mW cm^2)	References
$NiCo_2O_4$@CNTs	0.87 V@2 mA cm^{-2}	160	[1]
Co_3O_4/MnO_2	NA	43	[2]
$NiCo_2O_4$-rGO	0.70 V@5 mA mA cm^{-2}	125.3	[3]
α-MnO_2	0.8 V@10 mA mA cm^{-2}	140	[4]
α-MnO_2	0.85 V@10 mA mA cm^{-2}	166	[5]
MnO_2/CNTs	0.875 V@5 mA mA cm^{-2}	40.5	[6]
$NiCo_2O_4$@MnO_2-CNTs	0.8 V@20 mA mA cm^{-2}	255	[7]
$NiCo_2O_4$-CN	1.03 V@10 mA mA cm^{-2}	149.6	[8]
$NiCo_2O_4$@MnO_2/CNTs-Ni foam	0.69 V@5mA mA cm^{-2}	225	This work

NA: Not Available

REFERENCES

1. Chen C, Su H, Lu L, et al. Interfacing spinel $NiCo_2O_4$ and NiCo alloy derived N-doped carbon nanotubes for enhanced oxygen electrocatalysis. *Chem Eng J* 2021;408:127814. DOI: 10.1016/j.cej.2020.127814

2. Cui C, Du G, Zhang K, et al. Co_3O_4 nanoparticles anchored in MnO_2 nanorods as efficient oxygen reduction reaction catalyst for metal-air batteries. *J Alloys Compounds* 2020;814:152239. DOI: 10.1016/j.jallcom.2019.152239

3. Li Y, Cheng G, Zhou Z, et al. Shape-Controlled Synthesis of $NiCo_2O_4$-rGO as Bifunctional Electrocatalyst for Zn-Air Battery. *Chemelectrochem* 2019;6:4429-4436. DOI: 10.1002/celc.201901109

4. Xu N, Qiao J, Zhang X, et al. Morphology controlled $La_2O_3/Co_3O_4/MnO_2$-CNTs hybrid nanocomposites with durable bi-functional air electrode in high-performance zinc-air energy storage. *Appl Energy* 2016, 175: 495-504. DOI: 10.1016/j.apenergy.2016.04.036

5. Gu Y, Yan G, Lian Y, et al. Mn-III-enriched alpha-Mn_2 nanowires as efficient bifunctional oxygen catalysts for rechargeable Zn-air batteries. *Energy Storage Mater* 2019;23:252-260. DOI: 10.1016/j.ensm.2019.05.006

6. Xu N, Liu Y, Zhang X, et al. Self-assembly formation of Bi-functional Co_3O_4/MnO_2-CNTs hybrid catalysts for achieving both high energy/power density and cyclic ability of rechargeable zinc-air battery. *Sci Rep* 2016;6:33590. DOI: 10.1038/srep33590

7. Xu N, Cai Y, Peng L, et al. Superior stability of a bifunctional oxygen electrode for primary, rechargeable and flexible Zn-air batteries. *Nanoscale* 2018;10(28):13626-13637. DOI: 10.1039/c8nr03162b

8. Li P, Hu C, You T, et al. Development and characterization of bi-functional air electrodes for rechargeable zinc-air batteries: Effects of carbons. *Carbon* 2017;111:813-821. DOI: 10.1016/j.carbon.2016.10.057